REFERENCES

Ted Mao, David C.S. Kuhn, and Honghi Tran. (1997). Spread and Rebound of Liquid Droplets upon Impact on Flat Surfaces. AIChE Journal, 43(9), 2169-2179.

Xiaoguang Zhang, and Osman A. Basaran. (1997). Dynamic Surface Tension Effect in Impact of a Drop with a Solid Surface. Journal of Colloid and interface science, 187, 166-178.

N. Mourougou-Candoni, B. Prunet-Foch, F. Legay, M. Vignes-Adler, K. Wong. (1997). Influence of Dynamic Surface Tension on the Spreading of Surfactant Solution Droplets Impacting onto a Low-Surface-Energy Solid Substrate. Journal of Colloid and interface science, 192, 129-141.

R. Rioboo, M. Marengo, and C. Tropea. (2002). Time Evolution of Liquid drop impact onto solid, dry surfaces. Experiments in Fluids, 33, 112-124.

R. Rioboo, C. Bauthier, J. Conti, M. Voué, and J. De Coninck. (2003). Experimental Investigation of splash and crown formation during single drop impact on wetted surfaces. Experiments in Fluids, 35, 648-652.

F. Gentner, R. Rioboo, J.P. Baland, J. De Coninck. (2004). Low Inertia Impact Dynamics for Nanodrops. Langmuir, 20, 4748-4755.

R. Rioboo, C. Tropea. (2001). Outcome from a drop impact on solid surfaces. Journal article, 11(2), 155-165.

Abdullatif M. Alterraifi, Dalai Sherif, Abdelsamie Moet. (2003). Interfacial effects in the spreading of liquid droplets on solid substrates. Journal of Colloid and Interface Science, 264, 221-227.

R. Rioboo, M. H. Adão, M. Voué, J. De Coninck. (2006). Experimental evidence of liquid drop break-up in complete wetting experiments. Journal of Material Science, 41(16), 5068-5080.

M. Voué, R. Rioboo, C. Bauthier, J. Conti, M. Charlot, J. De Coninck. (2003). Dissipation and moving contact lines on non-rigid substrates. Journal of the European Ceramic Society, 23(15), 2769-2755.

Š. Šikalo, C. Tropea, E.N. Gannić. (2005). Impact of droplets onto inclined surfaces. Journal of Colloid and Interfacial science, 286, 661-669.

Zhao Yu, Tang Ge, L.-S. Fan. (2006). Multiscale simulation of oblique collisions of droplet on a surface in the Leidenfrost regime. Chemical Engineering science.

Hatta, N., Fujimoto, H., Kinoshita, K., Takuda, H. (1997). Experimental studies of deformation mechanism of a water droplet impinging on hot metallic surfaces above the Leidenfrost temperature. Journal of Fluid Engineering, 119, 692-699.

Fukai, J., Zhao, Z., Poulikakos, D., Megaridis, C. M., Miyatake, O. (1993), Modeling of the deformation of a liquid droplet impinging upon a flat surface, Phys. Fluids 5, 2588.

APPENDICES

System calibration

In order to calibrate high speed solid state CCD Camera, 4 methods of calibration must be applied (Ball calibration, Needle Calibration, Pendant drop calibration, and sessile drop calibration). The objective of calibration is to align CCD camera perpendicular to light system and object.

Appendix A Ball Calibration

A1 Ball Calibration

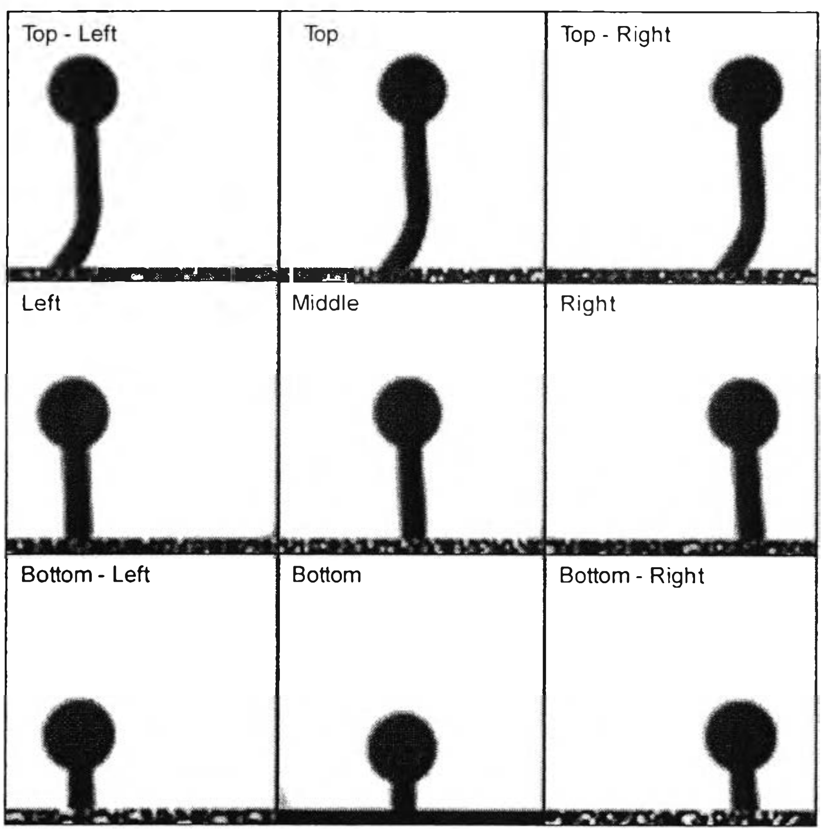

Figure A1 Iron ball (2 mm-diameters) on inverse needle and 9 different positions (Top, Top-Left, Top-Right, Middle, Left, Right, Bottom, Bottom-Left, and Bottom-Right).

The iron ball images are fit by program in order to indentify "H position" of iron ball image. After that, COEDG.BAT and SPH3.BAT is complied in C++ program in order to fit curve to calculate "Center of sphere", "sphere radius", "Aspect Ratio", and Standard error.

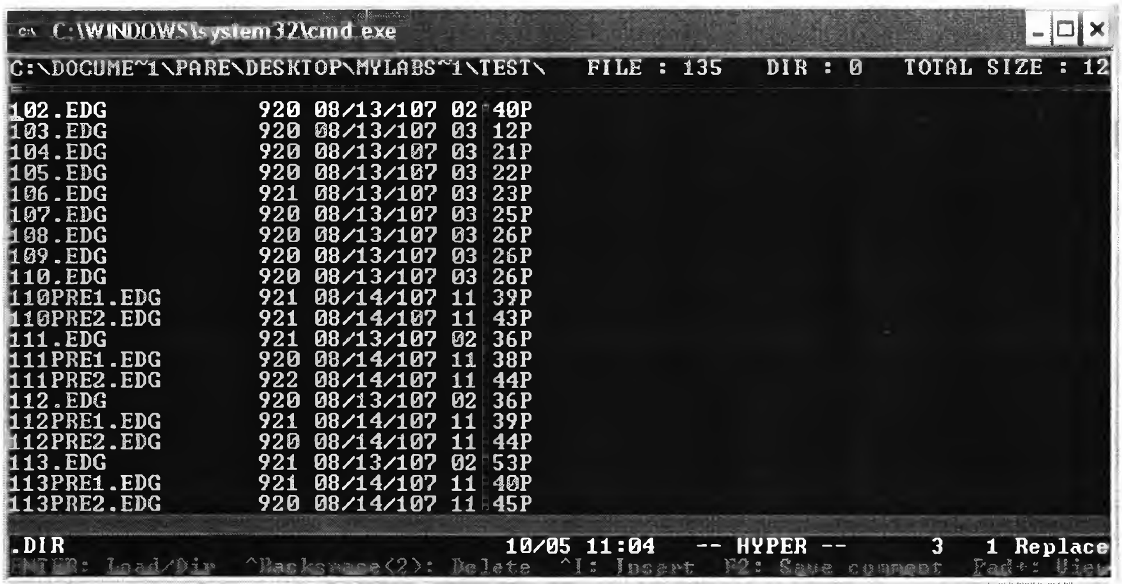

Figure A2 COEDG program interface.

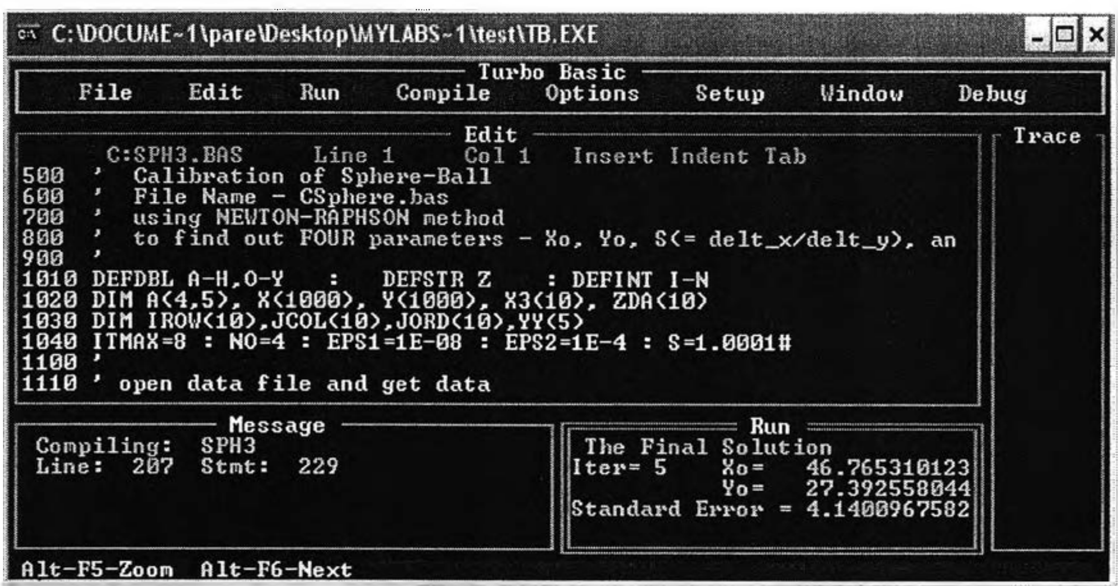

Figure A3 SPH3.BAT program interface.

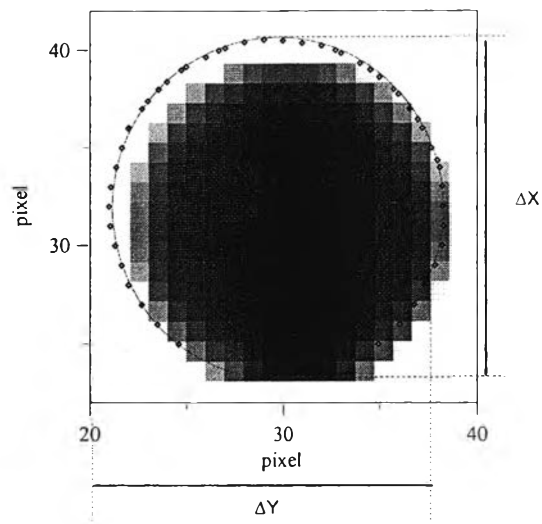

Figure A4 Curve fitting of iron ball.

In order to calibrate by using iron ball, the accuracy of value must be set within 3 digits.

Table A1 5 position of iron ball calibration results (1.Top, 2.Middle, 3.Bottom, 4.Left, and 5.Right).

1. Top

Top	x	y	Radius	Aspect Ratio	STD
110	28.73	36.38	8.3267	0.9852	0.0408
111	28.70	36.38	8.2923	0.9812	0.0381
112	28.71	36.38	8.3001	0.9834	0.0390
113	28.67	36.38	8.2551	0.9789	0.0394
114	28.70	36.38	8.2854	0.9817	0.0378
AVG			8.2919	0.9821	0.0390
STDEV			0.0259	0.0024	0.0012

2. Middle

Middle	x	y	Radius	Aspect Ratio	STD
110	29.75	29.45	8.3473	0.9856	0.0265
111	29.72	29.45	8.3152	0.9822	0.0255
112	29.73	29.45	8.3331	0.9846	0.0253
113	29.74	29.45	8.3440	0.9848	0.0271
114	29.71	29.45	8.3151	0.9824	0.0281
AVG			8.3309	0.9839	0.0265
STDEV			0.0154	0.0015	0.0012

3. Bottom

Bottom	x	y	Radius	Aspect Ratio	STD
115	31.62	19.25	8.3163	0.9858	0.0449
116	31.63	19.25	8.3365	0.9887	0.0472
117	31.63	19.25	8.3412	0.9879	0.0429
118	31.63	19.25	8.3381	0.9874	0.0433
119	31.67	19.24	8.3560	0.9815	0.0438
AVG			8.3376	0.9863	0.0444
STDEV			0.0142	0.0029	0.0017

4. Left

Left	x	y	Radius	Aspect Ratio	STD
100	18.73	27.23	8.3074	0.9868	0.0249
101	18.79	27.23	8.3839	0.9845	0.0243
102	18.76	27.23	8.3489	0.9801	0.0237
103	18.81	27.22	8.4097	0.9845	0.0225
104	18.79	27.22	8.3935	0.9826	0.0226
AVG			8.3687	0.9837	0.0236
STDEV			0.0409	0.0025	0.0010

5. Right

Right	x	y	Radius	Aspect Ratio	STD
125	44.65	26.34	8.3457	0.9855	0.0380
126	44.66	26.34	8.3527	0.9868	0.0374
127	44.70	26.33	8.3868	0.9896	0.0414
128	44.70	26.34	8.3843	0.9907	0.0408
129	44.66	26.34	8.3444	0.9876	0.0360
AVG			8.3628	0.9880	0.0387
STDEV			0.0210	0.0021	0.0023

A2 Ball Calibration results

The average value of "Middle" and "Bottom" position are used to find real scale and aspect ratio since middle and bottom are the most use position in the experiment.

Middle	Radius (pixel)	Aspect Ratio	STD
1	8.3309	0.9839	0.0265
2	8.3621	0.9859	0.0284
3	8.3256	0.9848	0.0253
Average	8.3395	0.9849	0.0267

Bottom	Radius (pixel)	Aspect Ratio	STD
1	8.3376	0.9863	0.0444
2	8.3570	0.9839	0.0413
3	8.3309	0.9864	0.0368
Average	8.3419	0.9855	0.0408

Ball diameter (mm) = 2.0000

Ball diameter (pixels) = 16.6814

Aspect Ratio = 0.9852

Real Scale (mm/pixel) = 0.1199

Appendix B Needle Calibration

The needle calibration is used to verify whether results from ball calibration are correct. The calibration step is;

a) Place needle in vertical direction perpendicular to the horizontal line.

b) Take 3 images at different time period without moving needle.

c) Repeat step a) and b) but place needle in horizontal direction.

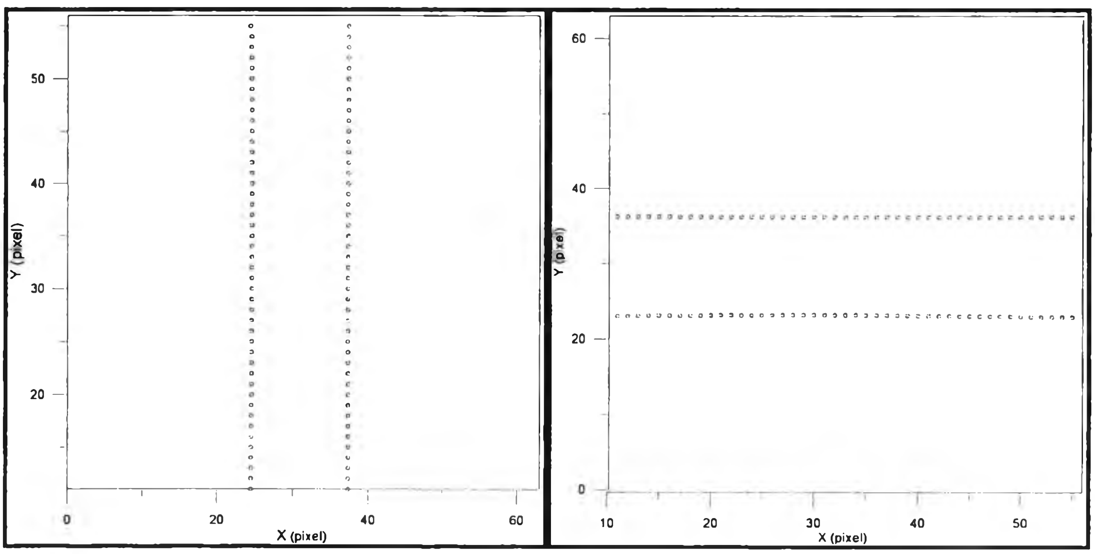

Figure B.1 Plot data of needle both in vertical and horizontal direction.

Three positions are used in the calibration Horizontal-Middle, Horizontal-Middle, and Vertical-Middle because these 3 positions are the most use area in the experiment.

Table B1 Needle calibration results.

	Diameter (pixel)	STDEV
Horizontal - Middle (Δy)	13.0959	0.0934
	13.0969	0.0819
	13.1068	0.0676
average	**13.0999**	**0.0810**

Horizontal – Bottom (Δy)	**13.0721**	**0.0409**
	13.0742	0.0413
	13.0735	**0.0401**
average	**13.0733**	**0.0408**
Vertical – Middle (Δx)	**12.8080**	**0.0663**
	12.8982	0.0988
	12.8606	**0.1076**
average	**12.8556**	**0.0909**

Needle diameter (mm) = 1.4700

Aspect Ratio = 0.9824

Real Scale x-direction (mm/pixel) = 0.1123

Real Scale in y-direction (mm/pixel) = 0.1143

Appendix C Pendant Drop Calibration

After ball and needle calibration, the pendant drop of water and acetone is used to verify since the pendant drop is close to the real experiment more than iron ball and needle.

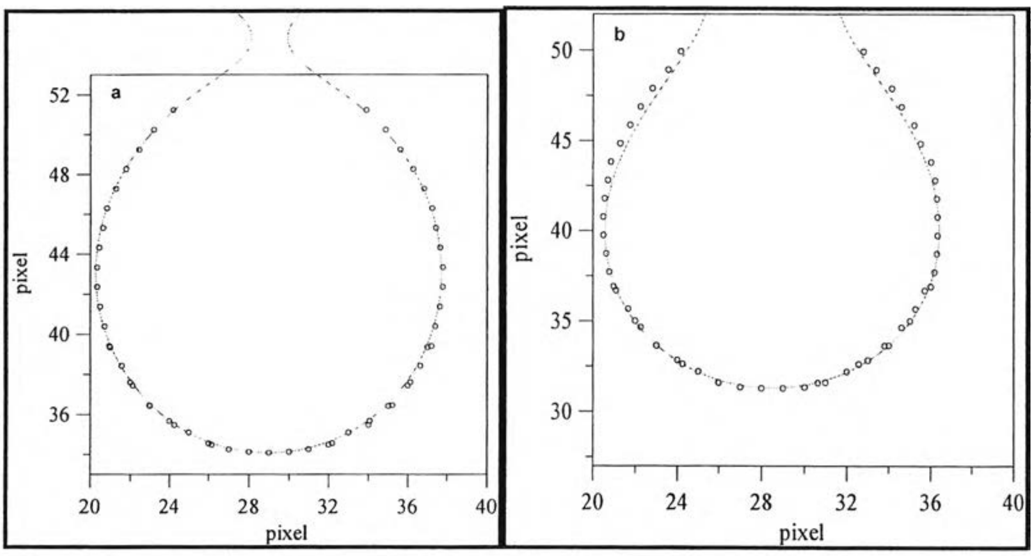

Figure C1 Pendant drop plot of a) Water and b) Acetone

Pendant drop surface tension is measured but fitting curve from plot data by MEG.BAT program. This program will calculate surface tension, surface area, drop volume.

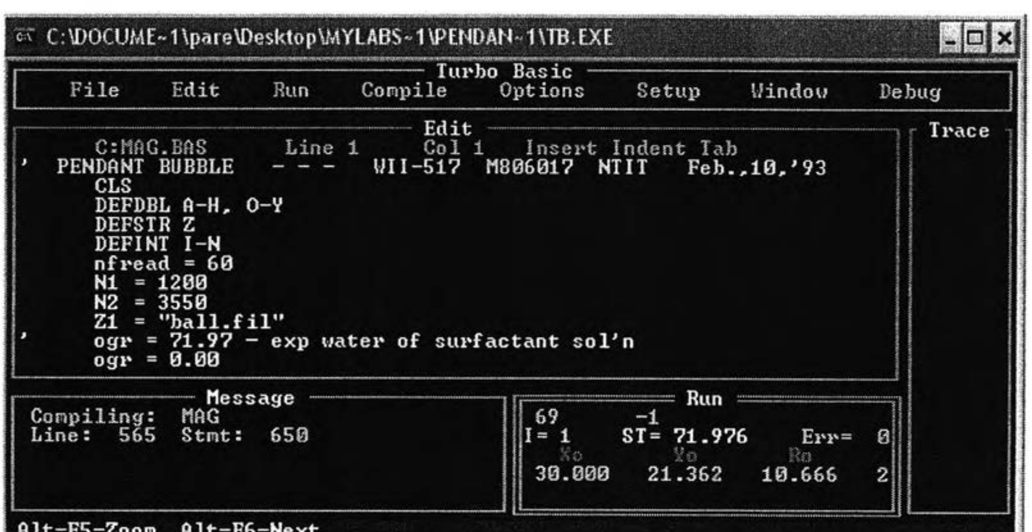

Figure C2: MEG.BAT program interface.

Table C1 Water pendant drop results.

Image no.	Surface Tension	radius (pixel)	β	X_{apex}	y_{apex}	Surface Area (mm^2)	Volume (mm^3)
100	71.930	9.977	-0.173	32.000	31.786	17.618	7.275
101	71.860	10.135	-0.179	31.000	30.466	18.201	7.671
102	71.956	10.086	-0.177	39.000	30.021	17.199	7.387
103	71.999	10.095	-0.177	38.000	30.043	17.205	7.403
104	71.982	10.081	-0.176	38.000	30.026	17.187	7.377
105	71.940	9.850	-0.168	39.000	31.932	16.109	6.771
106	71.911	9.854	-0.169	39.000	31.919	16.125	6.782
107	71.940	9.850	-0.168	39.000	31.930	16.714	6.896

The target of pendant drop calibration is to measure surface tension of water and acetone. If surface tension is close to the reference that means CCD camera alignment is in a correct position. The reference surface tension value of water and acetone at 20 °C and 1 atm are 72.8 and 23.7 respectively.

Table C2 Acetone pendant drop results.

Image no.	Surface tension	Radius (pixel)	β	X_{apex}	Y_{apex}	Surface area (mm^2)	Volume (mm^3)
100	23.081	7.492	-0.304	31.000	30.578	10.237	3.507
101	23.001	7.503	-0.306	30.000	29.472	10.781	3.654
102	22.957	7.543	-0.310	33.000	33.764	11.142	3.782
103	22.979	7.523	-0.308	33.000	33.617	11.153	3.760
104	23.018	7.458	-0.302	29.000	30.250	10.769	3.602

Appendix D Sessile Drop Calibration

Water is used as a tested liquid in sessile drop calibration. Water sessile drop on parafilm surface has contact angle between 105-120 degree depends on the wrap quality of parafilm on acrylic surface.

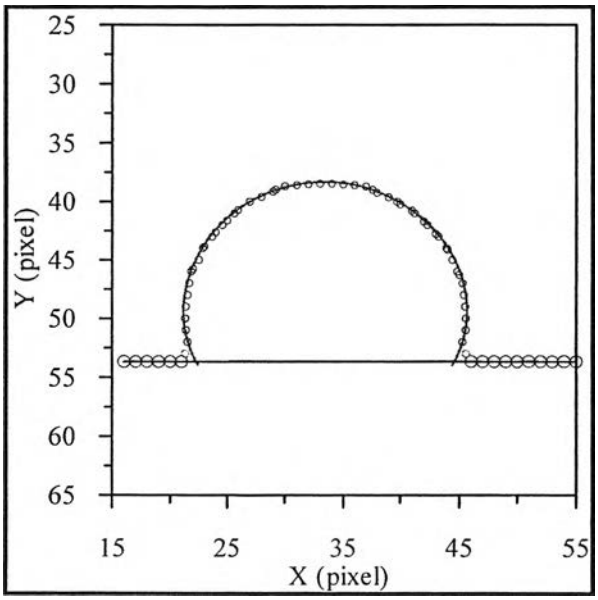

Figure D1 SS.BAT results of water sessile drop on parafilm wax surface.

In this calibration SS.BAT program is complied to calculate sessile drop contact angle (both left and right contact angle).

Figure D1 SS.BAT results program interface of water sessile drop on parafilm wax surface.

The water sessile drop is showed on the table below.

Table D1 Water sessile drop on parafilm wax surface.

Water Sessile drop on parafilm wax surface	
STC	25.076
Radius (pixel)	14.7552
β	1.0967
Left contact angle	113.452
Right contact angle	113.452
X_{apex}	34.007
Y_{apex}	38.692
STD	0.14703
Temp	25
Left plate	53.6785±0.0048
Right plate	53.6656±0.0093
Plate different	0.01294

Because parafilm surface can be stretched which affect to the water contact angle the water contact angle is vary depend on the warp quality of parafilm wax surface.

CURRICULUM VITAE

Name: Mr. Patrapee Arcade

Date of Birth: January 13th, 1981

Nationality: Thai

University Education:

2000-2004 Bachelor Degree of Chemical Engineering, Department of Chemical Technology, Faculty of Science, Chulalongkorn University, Bangkok, Thailand

Working Experience:

2004-2006 Position: Process Engineer

Company name: Siam Mitsui PTA co., Ltd

Presentations:

1. Chavadej, S Y, Lin. (2008, April 23) Water droplet impact phenomena onto super-hydrophobic surface. Paper presented at The 14th Symposium on Petroleum, Petrochemicals, and Polymers, Bangkok, Thailand.